Igf1r$^+$/CD34$^+$ immature ICC are putative adult progenitor cells, identified ultrastructurally as fibroblast-like ICC in Ws/Ws rat colon

X.Y. Wang [a], E. Albertí [b, c], E.J. White [a], H.B. Mikkelsen [d], J.O. Larsen [e], M. Jiménez [b], J.D. Huizinga [a, *]

[a] *Farncombe Family Digestive Health Research Institute, Department of Medicine, McMaster University, Hamilton, Ontario, Canada*
[b] *Department of Cell Biology, Physiology and Immunology, Universitat Autònoma de Barcelona, Barcelona, Spain*
[c] *Centro de Investigación Biomédica en Red de enfermedades hepáticas y Digestivas (CIBERehd)*
[d] *Department of Cellular and Molecular Medicine, University of Copenhagen, The Panum Institute, Copenhagen, Denmark*
[e] *Department of Neuroscience and Pharmacology, University of Copenhagen, The Panum Institute, Copenhagen, Denmark*

Received: July 29, 2008; Accepted: January 23, 2009

Abstract

The colon of Ws/Ws mutant rats shows impairment of pacemaker activity and altered inhibitory neurotransmission. The present study set out to find structural correlates to these findings to resolve mechanisms. In the colon of Ws/Ws rats, interstitial cells of Cajal associated with Auerbach's plexus (ICC-AP) were significantly decreased and ICC located at the submuscular plexus and intramuscular ICC were rarely observed based on immunohistochemistry and electron microscopy. Ultrastructural investigations revealed that there was no overall loss of all types of interstitial cells combined. Where loss of ICC was observed, a marked increase in fibroblast-like ICC (FL-ICC) was found at the level of AP. Immunoelectron microscopy proved FL-ICC to be c-Kit$^-$ but gap junction coupled to each other and to c-Kit$^+$ ICC; they were associated with enteric nerves and occupied space normally occupied by ICC in the wild-type rat colon, suggesting them to be immature ICC. In addition, a marked increase in immunoreactivity for insulin-like growth factor 1 receptor (Igf1r) occurred, co-localized with CD34 but not with c-Kit. A significantly higher number of Igf1r$^+$/CD34$^+$ cells were found in Ws/Ws compared to wild-type rat colons. These CD34$^+$/Igf1r$^+$ cells in the Ws/Ws colon occupied the same space as FL-ICC. Hence we propose that a subset of immature ICC (FL-ICC) consists of adult progenitor cells. Immunohistochemistry revealed a reduction of neurons positive for neuronal nitric oxide synthase. The functional capabilities of the immature ICC and the regenerative capabilities of the adult progenitor cells need further study. The morphological features described here show that the loss of pacemaker activity is not associated with failure to develop a network of interstitial cells around AP but a failure to develop this network into fully functional pacemaker cells. The reduction in nitrergic innervation associated with the Ws mutation may be the result of a reduction in nitrergic neurons.

Keywords: interstitial cells of Cajal • Ws/Ws rat • colon

Introduction

Our understanding of the role of interstitial cells of Cajal (ICC) in control of gastrointestinal motility has been facilitated greatly by studying mice and rats which harbour a mutation in the *c-kit* gene that results in abnormal development of subtypes of ICC. In the intestine it has provided strong evidence for a pacemaker function of ICC associated with Auerbach's plexus (ICC-AP), in intestinal tissues without ICC-AP, no electrical slow wave activity was observed [1, 2]. This was substantiated by studies on isolated ICC which showed rhythmic pacemaker currents whereas isolated smooth muscle cells did not [3, 4]. *In vivo*, the absence of ICC pacemaker cells markedly affects intestinal motility with the regular rhythmic anally directed peristalsis replaced by disorganized contractile activity [5]. Further studies showed that the intestinal musculature in *W* mutant animals, in response to stretch or distention can produce rhythmic propagating contractions in the absence of ICC [6], clearly indicating that the musculature harbours a backup system to generate propulsive contractile activity. In the absence of ICC, the musculature can be paced by external stimuli and the regulation

*Correspondence to: Dr J.D. HUIZINGA,
Department of Medicine,
Farncombe Family Digestive Health Research Institute,
McMaster University, Hamilton, L8N3Z5, Ontario, Canada.
Tel.: 905-525-9140 ext. 22590
Fax: 905 522 3454
E-mail: huizinga@mcmaster.ca

doi:10.1111/j.1582-4934.2009.00689.x

of contraction frequency is clearly different [7]. As outlined above, most of the evidence for a role of ICC has been obtained in the small intestine, although the earliest studies showing a relationship between physical removal of ICC and loss of pacemaker activity were carried out in the canine colon [8–10]. The canine colon, however, is not a good model for human colonic motility and it is highly relevant to study the role of ICC in other models [11]. The rat colon has provided us with data suggesting that ICC-AP are associated with regular rhythmic depolarizations at 1.2 cycles/min. [12, 13] and that ICC associated with the submuscular plexus (ICC-SMP) may provide a pacemaker function associated with fast rhythmic depolarizations at 20 cycles/min. [13]. In the Ws/Ws colon, this high-frequency pacemaker activity was not evident [12] and the present study provides support for the hypothesis that absence of ICC-SMP is responsible for this.

The role of ICC in innervation is more controversial. Evidence for a role of ICC in mediating nitrergic innervation to the musculature was obtained using the W/W^v stomach [14]. This led to a hypothesis that nitric oxide would not effectively diffuse from varicosities to smooth muscle cells suggesting that ICC were essential in nitrergic innervation [15]. Subsequently studies appeared that showed evidence in support of [16, 17] or against [18, 19] the hypothesis. The role of ICC in innervation of the gut is likely to be very important but it should primarily be viewed as innervation of ICC to modify ICC function and thereby indirectly affecting smooth muscle activity. Controversies in interpretation have been due in part to our limited understanding of consequences of the *W* mutation on gut structure and function other than partial loss of ICC. This is particularly true for the colon, where we studied pacemaker activity and inhibitory innervation of wild-type and Ws/Ws rats [12]. We observed marked impairment of pacemaker activity which could have been due to loss of pacemaker ICC. We also observed a reduction in inhibitory nitrergic innervation which could have been due to loss of intramuscular ICC (ICC-IM) or loss of nitrergic nerves. The present study set out to investigate structural and immunohistochemical features of interstitial cells and nitrergic nerves that would give evidence for or against these hypotheses. In addition, we suggested that if loss of ICC was to be found, this might be due not to loss of cells but to the presence of immature ICC: immature ICC present at birth [20] might develop without further differentiation. In addition we sought evidence for the hypothesis that all or some of these immature ICC might have features of ICC progenitor cells as deduced from studies on the murine stomach [21]. We were also interested in the relationship between potential progenitor cells based on immunohistochemistry and fibroblast-like ICC (FL-ICC) as identified by ultrastructural studies in the rat stomach [22].

Material and methods

Animals and tissue preparation

Ten Ws/Ws and sibling wild-type rats of both sexes and over 10 weeks old were used in the present study. After the animals were decapitated, the entire colon was removed. Colon was washed in phosphate buffered saline (PBS) and divided into three different parts: proximal, mid and distal as previously described [23]. The housing and handling of animals were approved either by the McMaster University Animal Care Committee and the Canadian Council on Animal Care or by The Ethics Committee of the Universitat Autonoma de Barcelona.

Immunohistochemistry for c-Kit, neuronal nitric oxide synthase (nNOS), insulin-like growth factor 1 receptor (Igf1r), CD34 and protein gene product 9.5 (PGP 9.5)

Both the proximal, mid and distal colon segments were prepared for frozen sections and musculature whole-mount preparations, respectively. All whole-mount specimens were prepared under the dissection microscope by peeling the mucosa and submucosa with sharp dissection tool. For frozen section preparations, tissues were embedded in Tissue-Tek (Miles Lab., Haperville, IL, USA) and frozen in isopentane in a beaker submerged in liquid nitrogen. Frozen sections measuring 8 μm were cut with the cryostat and mounted on the coated slides. Both whole mounts and frozen sections were fixed in 4% paraformaldehyde for 10 min. and then used to assess the distribution of c-Kit, nNOS, Igf1r, CD34 and PGP 9.5^+ cells in the musculature of rat colon. After blocking the non-specific binding in 5% normal goat serum or 2% albumin bovine serum (BSA), tissues were incubated overnight at room temperature in primary antibodies, which were rabbit anti-c-Kit 1:200 (Dakocytomation, Glostrup, Denmark); rabbit anti-nNOS 1:500 (Chemicon, Temecula, CA, USA); goat anti-Igf1r (IGF-IRα (L-15) 1:100 (Santa Cruz Biotech., Santa Cruz, CA, USA), rabbit anti-CD34 1:100 (Santa Cruz Biotech.) and rabbit anti-PGP 9.5 1:2500 (Chemicon). For light microscopy, secondary antibody was biotin conjugated goat anti-rabbit IgG and Vectastain ABC Kit (Vector Laboratories, Burlingame, CA, USA). Three 3′ diaminobenzidine (0.05%) plus 0.01% H_2O_2 in 0.05M Tris buffer saline (pH 7.6) were used as a peroxidase substrates. For fluorescence microscopy (double labelling staining with c-Kit/Igf1r, Igf1r/CD34 and Igf1r/PGP 9.5), secondary antibodies were either Cy3 conjugated donkey anti-goat IgG/Cy2 conjugated donkey anti-rabbit IgG or Cy3 conjugated donkey anti-rabbit IgG/Cy2 conjugated donkey anti-goat IgG.

All the antibodies were diluted in 0.2% BSA in 0.05M PBS (pH 7.4) + 0.3% triton-X-100. Negative controls included the omission of primary or secondary antibodies from the incubation solution. All the immunostaining were examined either using a conventional microscope with an attached digital camera (Sony 3CCD, Model # DXC-930, Tokyo, Japan) or a confocal microscope (Zeiss LSM 510, Göttingen, Germany) with excitation wavelengths (488 nm and 595 nm) appropriate for Cy2 and Cy3.

Quantification of Igf1r, Igf1r/CD34 and Igf1r/PGP 9.5 immunoreactivities

Quantification on the frozen sections was performed with Photoshop, version 7.0 (Adobe Systems; Mountain View, CA, USA). Fifty sections immunostained with Igf1r or double labelled with Igf1r/CD34 and Igf1r/PGP 9.5 were chosen, respectively. Immunopositivity was identified and highlighted using density slicing on colour scale images. The area with either single labelled or double labelled immunoreactivity on each picture was measured and expressed as percentage of total area. Regions with increased background staining, occasionally found at the borders of the

image, were excluded from the analysis. Another 'background' feature was the Igf1r immunoreactivity found on enteric nerves in wild-type as well as Ws/Ws rats; this was to be expected since insulin is a proven growth factor for nerves [24]. Values are expressed as mean ± S.E. Means were compared using Student's unpaired t-test. Data were considered statistically significant when $P < 0.05$.

Stereological analysis of nNOS immunoreactivity

An established stereological technique, the fractionator technique [25–27] was used to count the number of $nNOS^+$ cells in the proximal, mid and distal colon of both Ws/Ws and wild-type rats as previously described [23]. Briefly, whole-mount preparations were used to study the morphology and area density (number of cells/mm^2: see stereological analysis) of $nNOS^+$ cells. The counting was performed on systematic random fields of vision by moving an unbiased counting frame through the full thickness of the whole-mount specimen. The stereological analysis of $nNOS^+$ cells was carried out on a computer monitor using computer-assisted interactive stereological test systems (The CAST-grid software, Olympus, Glostrup, Denmark). The $nNOS^+$ cells were counted as one group through the entire thickness of the whole mount. Unpaired t-tests were used to determine differences between wild-type and Ws/Ws rats in each segment. ANOVA was used to compare proximal, mid and distal colon.

Conventional electron microscopy

Tissues from proximal, mid and distal colon of both Ws/Ws and wild-type rats were removed and fixed by immersion in 2.5% glutaraldehyde in 0.075 M sodium cacodylate buffer, pH 7.4, containing 4.5% sucrose and 1 mM $CaCl_2$ for 6 hrs at room temperature. After primary fixation, 1-cm-wide pieces were cut from each tissue and immersed in the same fixative for an additional fixation overnight at 4°C. Following fixation, all tissues were washed in 0.1 M cacodylate buffer, containing 6% sucrose and 1.24 mM $CaCl_2$ (pH 7.4) at 4°C. After washing, each piece was cut in circular and longitudinal strips. The tissue strips were post-fixed with 1% OsO_4 in 0.1 M cacodylate buffer (pH 7.4) at room temperature for 60 min., stained with saturated uranyl acetate for 30 min. at room temperature, dehydrated in graded ethanol and propylene oxide, and embedded in Epon-Araldite. Semi-thick sections (1 μm) were cut and stained with 1% toluidine blue for light microscopic examination. Following the examination of the toluidine blue stained sections, ultrathin sections were cut, mounted on grids and stained with lead citrate. The grids were examined in a JEOL-1200 EX Biosystem electron microscope (Jeol Ltd., Tokyo, Japan) at 80 kV.

Immunoelectron microscopy for c-Kit

Both wild-type and Ws/Ws colons were fixed by immersion in 4% paraformaldehyde, 0.1% glutaraldehyde and 0.2% picric acid in 0.1 M phosphate buffer (PB, pH 7.4) for 1 hr at room temperature. After a brief rinse in 0.1 M PB, tissue was washed vigorously at room temperature in several changes of 50% ethanol until the picric acid staining of the tissue had disappeared (about 20 min.). Vibro-sections of 150 μm were cut with a vibrotome (Lancer, series 1000, Lancer, Vibratome, St. Louis, MO, USA), washed in 0.11 yds PB and incubated in 0.1% $NaBH_3CN$ (Aldrich Chemical Co., Milwaukee, WI, USA) in 0.1 M PB for 15 min. at room temperature to increase the tissue permeability. Same immunostaining steps (ABC technique) as light microscopic immunohistochemistry were performed except that 0.3% triton-X-100 was taken out from 0.05 M PBS (pH 7.4). The tissue was checked by light microscopy to see if the reaction was suitable, prior to being post-fixed, block-stained, dehydrated, embedded and grid-stained with lead citrate for conventional electron microscope examination as mentioned above.

Results

Quantitative immunohistochemistry

In order to assess correlations between loss of electrical pacemaker activity [12] and ICC, c-Kit^+ ICC were examined. In proximal, mid and distal colons of wild-type rats, c-Kit immunohistochemical staining on frozen sections showed c-Kit^+ cells at the level of Auerbach's plexus (ICC-AP), the submuscular plexus (ICC-SMP) and within the musculature (ICC-IM). ICC-APs were abundant and connected to each other to form a dense network at the level of Auerbach's plexus (Fig. 1a, c and e). They usually surrounded the myenteric ganglia (Fig. 1a and c) and occasionally c-Kit^+ cells were observed protruding into the ganglia (Fig. 1c). c-Kit^+ ICC were also seen to extend into the circular and longitudinal muscle layers to connect with ICC-IM close to Auerbach's plexus (Fig. 1a). c-Kit^+ ICC-IM usually ran parallel to adjacent smooth muscle cells. c-Kit^+ cells were also concentrated at the level of the SMP at the border of the submucosa (Fig. 1a, c and e) and formed a local network (not shown, see [12]). In the proximal and mid colons of Ws/Ws rats (Fig. 1b and d), relatively few c-Kit^+ ICC-AP had developed, whereas hardly any ICC at the level of the SMP and within the muscle layers were encountered. There was hardly any c-Kit^+ reaction at any level in the distal colon of Ws/Ws rats (Fig. 1f).

In order to provide a possible explanation for an observed reduction of nitrergic neurotransmission in the Ws/Ws colon [12], $nNOS^+$ neurons were examined. $nNOS^+$ neurons were present between the circular and the longitudinal smooth muscle layers at the level of Auerbach's plexus forming a network of nerve strands with cell bodies in ganglia, in both wild-type (Fig. 2a–c) and Ws/Ws rats (Fig. 2d–f). $nNOS^+$ cells displayed dark somata and non-reacting nuclei. Myenteric ganglia were interconnected by $nNOS^+$ nerve strands of variable length and thickness. Regional differences were found between the three parts of the colon both in wild-type and Ws/Ws animals (Fig. 2g and h). The highest density of $nNOS^+$ cells (ANOVA $P < 0.05$) was found in the mid colon for both wild-type and mutant animals (Fig. 2g and h). The density of $nNOS^+$ cells was higher in wild-type rats than in Ws/Ws animals, with the exception of the proximal colon (Table 1).

In order to identify potential ICC progenitor cells [21], double labelling of c-Kit and Igf1r (Fig. 3a–l), Igf1r and CD34 (Fig. 4a–i) or Igf1r and PGP 9.5 (Fig. 5a–f) was carried out. In both wild-type and Ws/Ws rat colons, $Igf1r^+$ cells were found in areas where ICC reside. In wild-type tissue, they were mainly located at the level of Auerbach's plexus and moderately in the SMP and within smooth muscle layers (Fig. 3b and e). In Ws/Ws colon, $Igf1r^+$ cells were

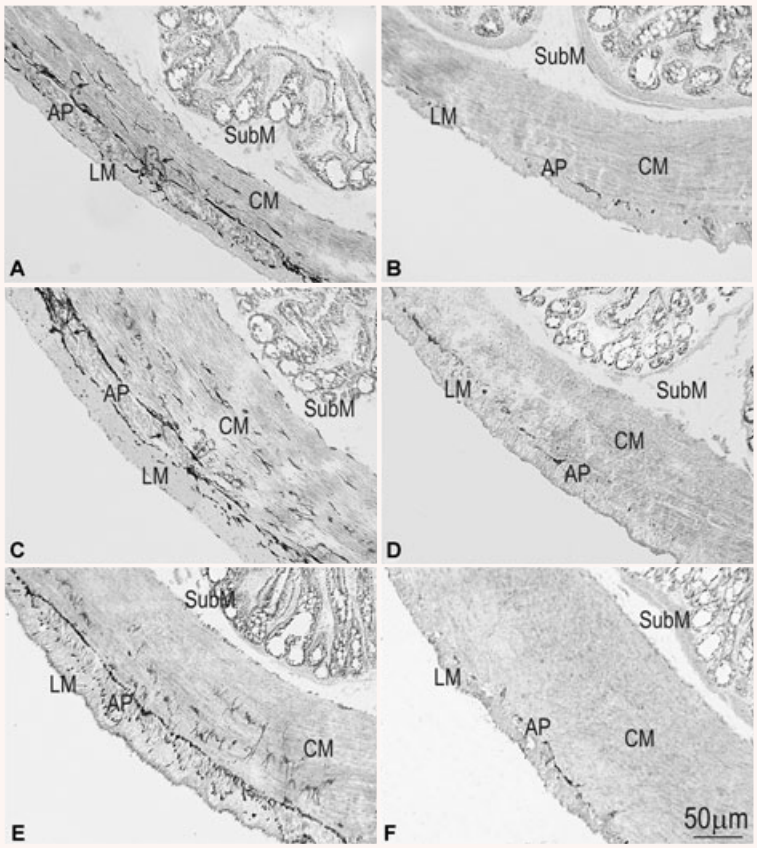

Fig. 1 Immunohistochemistry (frozen sections) showing c-Kit$^+$ cells in the proximal (**a** and **b**), mid (**c** and **d**) and distal (**e** and **f**) colon from wild-type (**a**, **c** and **e**) and Ws/Ws (**b**, **d** and **f**) rats. In wild-type rats (**a**, **c** and **e**) a high density of c-Kit$^+$ cells is observed at the level of the AP surrounding the ganglia, at the submucosal (SubM) border and within both circular (CM) and longitudinal muscle (LM) layers. Small arrows in figure a show ICC-AP connected with ICC-IM in the circular muscle layer and small arrows in (**c**) indicate the ICC-AP protruding into the myenteric ganglia. Mutant rats only showed a few c-Kit$^+$ cells at the AP region. Scale bar is for (**a**)–(**f**).

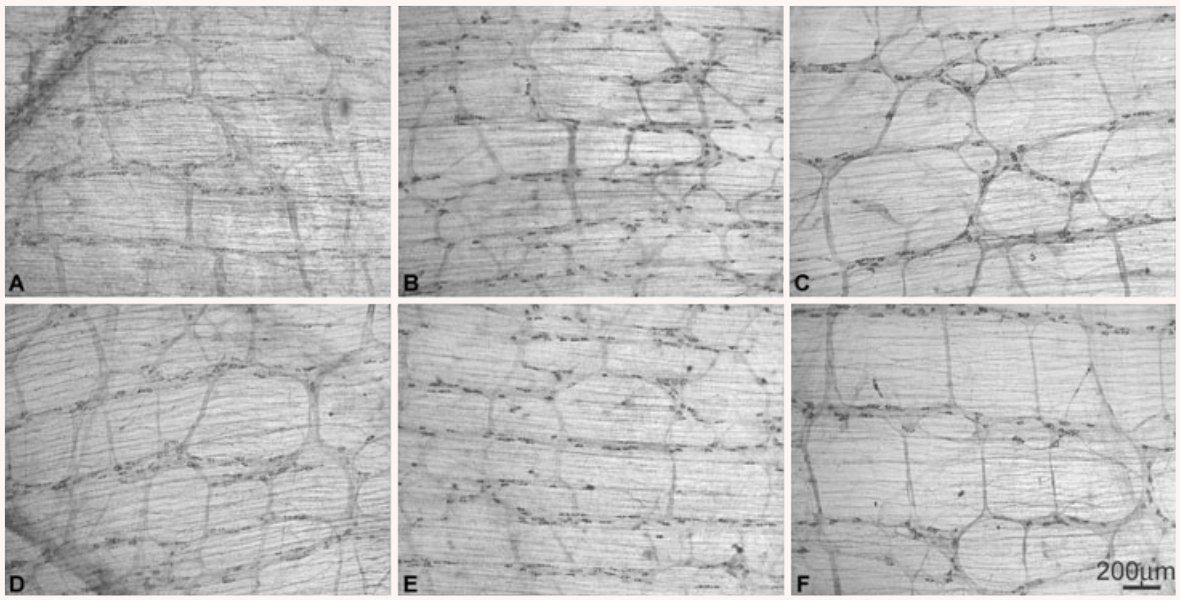

Fig. 2 Whole mount preparations showing nNOS$^+$ cells in the proximal, mid and distal colon from wild-type (**a**–**c**) and Ws/Ws (**d**–**f**) rats. Myenteric ganglia (G) were interconnected to each other by nerve strands.

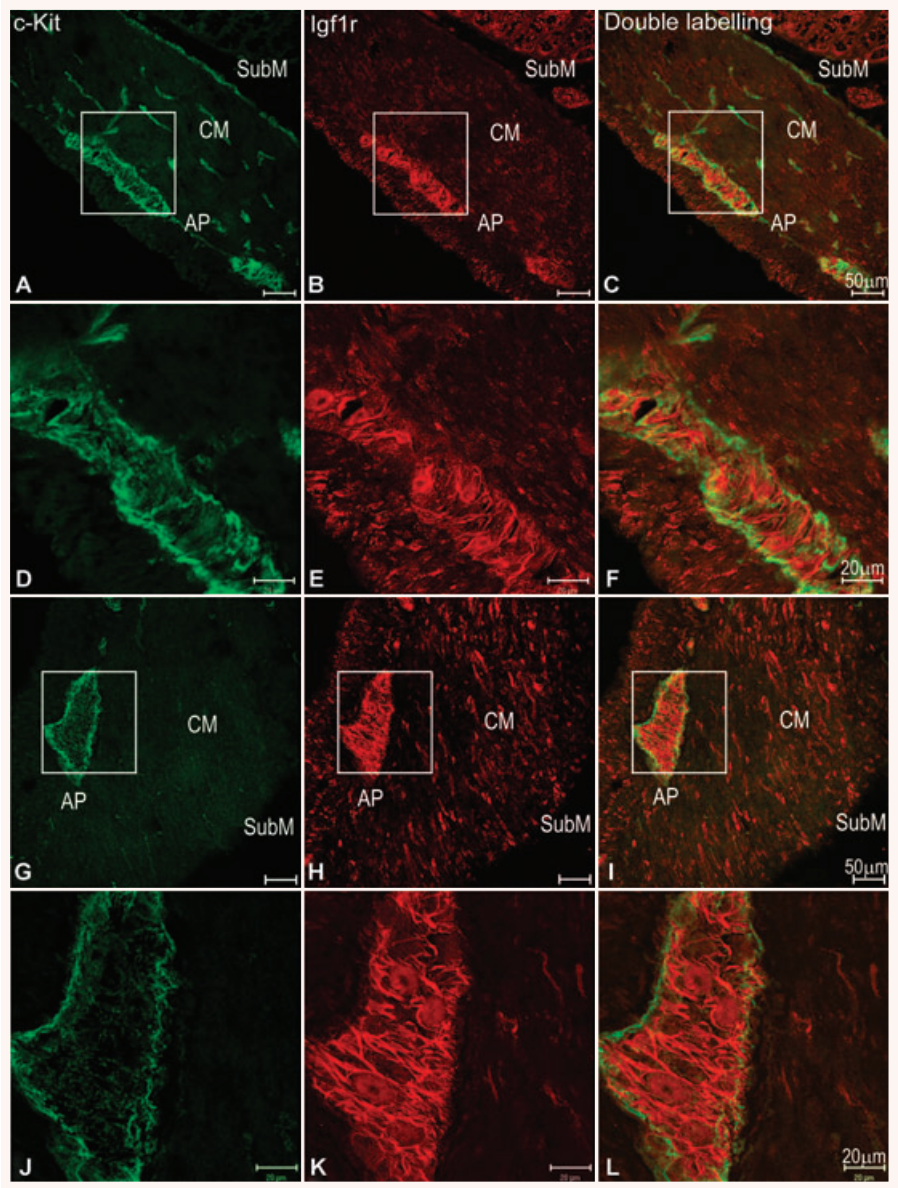

Fig. 3 Immunohistochemistry (frozen sections) showing double labelling of c-Kit /Igf1r positivities in wild-type (**a–f**) and Ws/Ws (**g–l**) mid colons. (**d**)–(**f**) and (**j**)–(**l**) are enlarged figures from the boxes in (**a**)–(**c**) and (**g**)–(**i**). In both wild-type and Ws/Ws colons, myenteric neurons showed relatively weak Igf1r positivity (**e** and **k**).There were many strongly reactive and spindle-shaped Igf1r$^+$ cells within the myenteric ganglia and scattered in the muscle layers. Both Igf1r$^+$ cells and ICC occur at the ganglia although there was no co-expression between Igf1r and c-Kit. In Ws/Ws colon, Igf1r$^+$ cells were greatly increased in number within the myenteric ganglia and especially in the circular muscle layers. CM: circular muscle cells; AP Auerbach's plexus; SubM: submucosa.

Table 1 Comparison of the density of nNOS$^+$ cells between wild-type and Ws/Ws rats in each part of the colon (raw data are expressed in Fig. 2). The coefficient of variation (CV) is calculated as the S.D. divided by the mean. The percentage of loss (%Loss = [wild-type − (Ws/Ws)] × 100/wild-type) was calculated using the area density in Ws/Ws rats and considering wild-type values as 100%. Unpaired t-test was used to estimate differences between wild-type and Ws/Ws rats in each segment.

	Colon	Wild-type ($n = 4$)	Ws/Ws ($n = 4$)	% loss	Significance
nNOS$^+$ cells at Auerbach's plexus	Proximal	53.7 ± 0.8	40.9 ± 1.3		n.s.
	Mid	138.6 ± 0.1	89.7 ± 0.5	35%	$P < 0.01$
	Distal	81.6 ± 0.3	57.6 ± 0.3	29%	$P < 0.05$

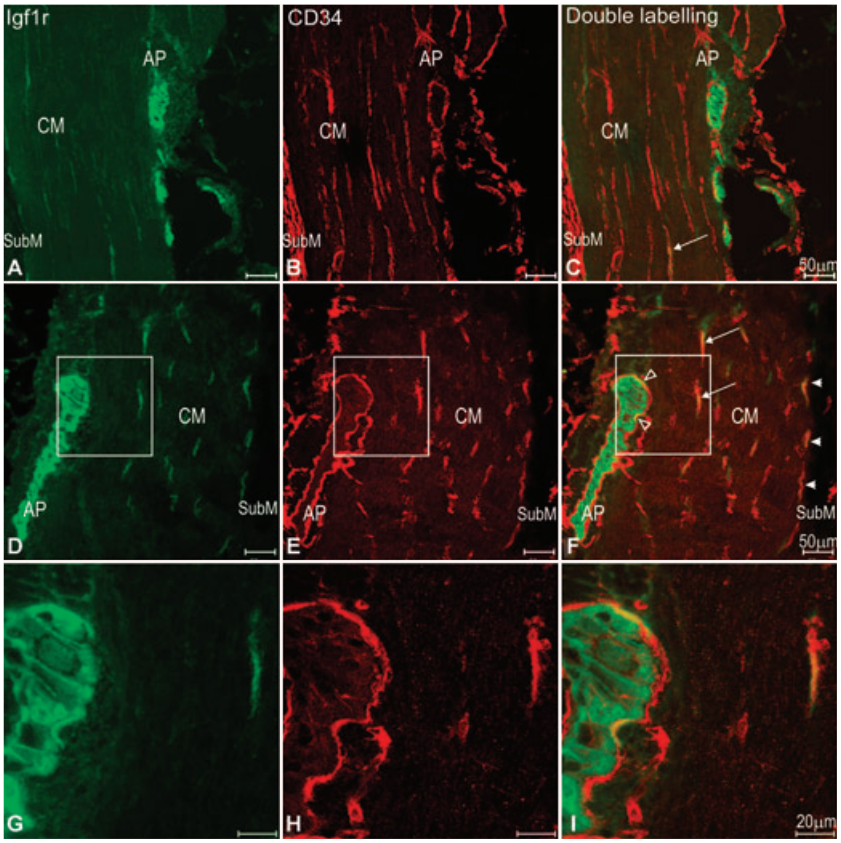

Fig. 4 Immunohistochemistry (frozen sections) showing double labelling of Igf1r/CD34 positivities in wild-type (**a**–**c**) and Ws/Ws (**d**–**i**) mid colons. The density of co-localization of Igf1r and CD34 was much higher in Ws/Ws colon (**d**–**i**) compared to wild-type colon (**a**–**c**). (**g**)–(**i**) are enlarged figures from the boxes in (**d**)–(**f**). The co-localized cells were found around the Auerbach's plexus (hollow arrow heads), within the muscle layers (arrows) and around the SMP (arrow heads). CM: circular muscle cells; AP Auerbach's plexus; SubM: submucosa.

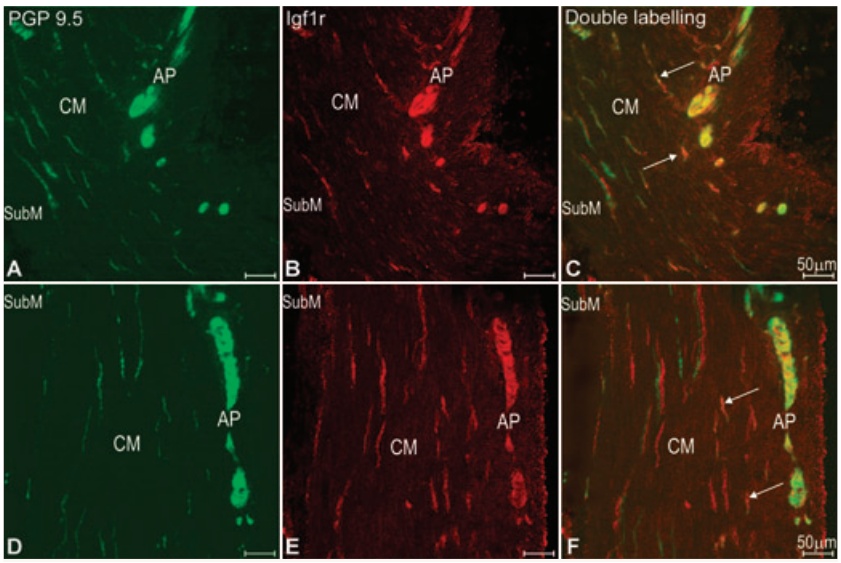

Fig. 5 Immunohistochemistry (frozen sections) showing double labelling of PGP 9.5 /Igf1r positivities in wild-type (**a**–**c**) and Ws/Ws (**d**–**f**) mid colons. The density of the Igf1r/PGP 9.5 co-expressed cells (arrows) was similar in wild-type and Ws/Ws colon. Some of the $Igf1r^{+}$, PGP 9.5^{-} cells were closely apposed to PGP 9.5^{+} enteric nerves. CM: circular muscle cells; AP Auerbach's plexus; SubM: submucosa.

greatly increased in all above locations (Figs 3h, k and 6). No co-expression of Igf1r and c-Kit was found (Fig. 3c, f, i and l) in both wild-type and Ws/Ws colons. Igf1r was found to be co-expressed with both CD34 (Fig. 4a–i) and PGP 9.5 (Fig. 5a–f). Only a fraction of the $CD34^{+}$ cells showed Igf1r immunoreactivity (Fig. 4a–f). In Ws/Ws colon (Fig. 4d–i), the co-expression of Igf1r/CD34 was markedly increased compared to wild-type colon (Figs 4a–c and 6, $P < 0.05$), and the co-expressed cells were found both around

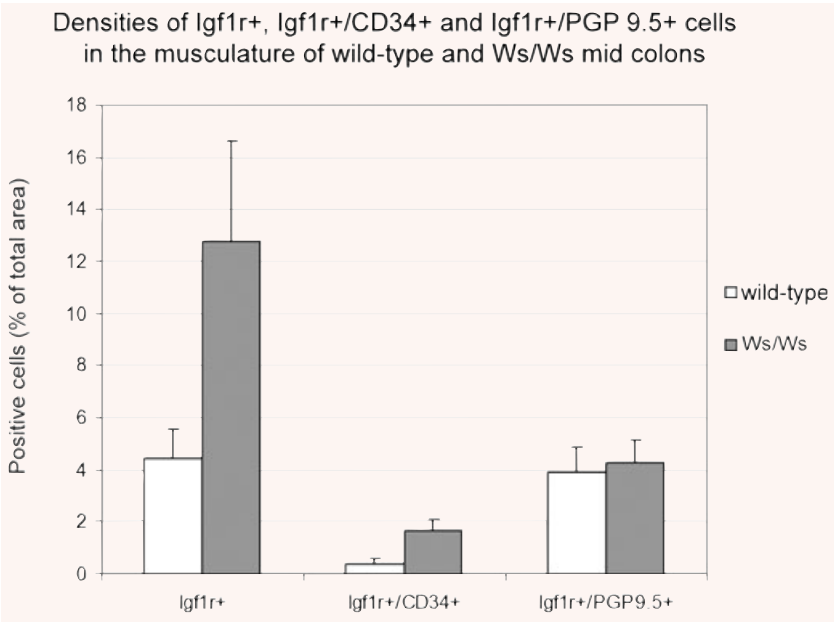

Fig. 6 Densities of Igf1r$^+$ cells in the whole musculature of wild-type and Ws/Ws rat mid colon. Compared to wild-type rat colon, Igf1r reactivity in Ws/Ws rat colon was significantly increased ($P = 0.021$, $n = 50$). Compared to wild-type rat colon, the density of Igf1r$^+$/CD34$^+$ cells was significantly increased in Ws/Ws rat colon ($P = 0.011$, $n = 50$); whereas the density of Igf1r$^+$/PGP 9.5+ cells was not increased in Ws/Ws colon ($P = 0.799$, $n = 50$).

Auerbach's plexus, within the muscle layers and close to the SMP (Fig. 4f). Co-localization of Igf1r/PGP 9.5 was found mostly in the Auerbach's plexus and moderately within the muscle layers; there was no difference in the degree of co-localization between wild-type and Ws/Ws rat colons (Figs 5a–f and 6, $P > 0.05$). Igf1r$^+$ cells were also found adjacent to enteric nerves (Fig. 5c and f).

Ultrastructure

The dominant interstitial cells associated with nerve structures in the wild-type and Ws/Ws colon were ICC, FL-ICC, fibroblasts and macrophage-like cells. The term FL-ICC was used in accordance with the studies of Ishikawa and co-workers in the Ws/Ws rat stomach [22]. No obvious difference in the density of all interstitial cells combined surrounding Auerbach's plexus and the SMP were seen comparing wild-type and Ws/Ws colon. Quantification in the Ws/Ws colon of the different subtypes was not attempted, because in many 'ICC' profiles a definite differentiation between ICC and FL-ICC could not be made since a major criterion used was the presence of caveolae, which cannot be decided upon studying only one profile. Using low magnification, many potential ICC according to their location, scarce perinuclear region and electron-dense cytoplasm, were observed both at the level of the Auerbach's plexus (Fig. 7b) and the SMP (Fig. 9b) of both wild-type and Ws/Ws colon. Using higher magnification, we established that the wild-type tissue was dominated by typical ICC identified by their abundant organelles, in particular mitochondria, presence of caveolae (Figs 7a, 9a and 10a), gap-junction contact with smooth muscle cells and close apposition to nerves (Fig. 10a). In the Ws/Ws colon, only a few ICC were present (Fig. 7c). FL-ICC were present in much higher number with an electron-dense cytoplasm and all other characteristics of ICC except that they had conspicuous rough endoplasmic reticulum and were without caveolae as identified in the profiles studied, similar to the FL-ICC in the Ws stomach [22]. Typical examples are shown in Figs 7d and 9c and d. These FL-ICCs occupied the typical position of ICC and they were seen to make contact with adjacent FL-ICC and smooth muscle cells (Figs 7d and 9d). They were also close to nerve structures but no special junction was found between them as they occur between ICC-IM and nerves. The differences between these FL-ICC and traditional fibroblasts (Figs 9c and 10b) were their higher electron density, the close connections with similar cells, ICC and/or smooth muscle cells and occupation of typical ICC sites.

At the level of Auerbach's plexus in the Ws/Ws colon, both typical ICC-AP (Fig. 7c) and FL-ICC (Fig. 7d) were observed. Immuno EM showed typical ICC to be c-Kit$^+$ (Fig. 8a and b) and FL-ICC to be c-Kit$^-$ (Fig. 8b). At the SMP of Ws/Ws colon, many interstitial cells were found associated with nerve structures (Fig. 9d). There were almost no typical and ultrastructurally defined ICC-SMP as in wild-type colon (Fig. 9a). Most of the interstitial cells in this region were FL-ICC (Fig. 9b–d), which were connected to each other (Fig. 9d). In many profiles, the only feature different from typical ICC was an absence of caveolae (Fig. 9c). Fibroblasts (Fig. 9c) and macrophage-like cells (not shown) were also observed at the level of the SMP.

Most nerve structures within the circular and longitudinal muscle layer of the Ws/Ws colon were associated with interstitial cells. However, positively identifiable ICC-IM were not found in mutant rats. FL-ICC, with gap junctions between each other or with smooth muscle cells, were also not identified at this level. Mostly, the nerve structures were associated with fibroblasts

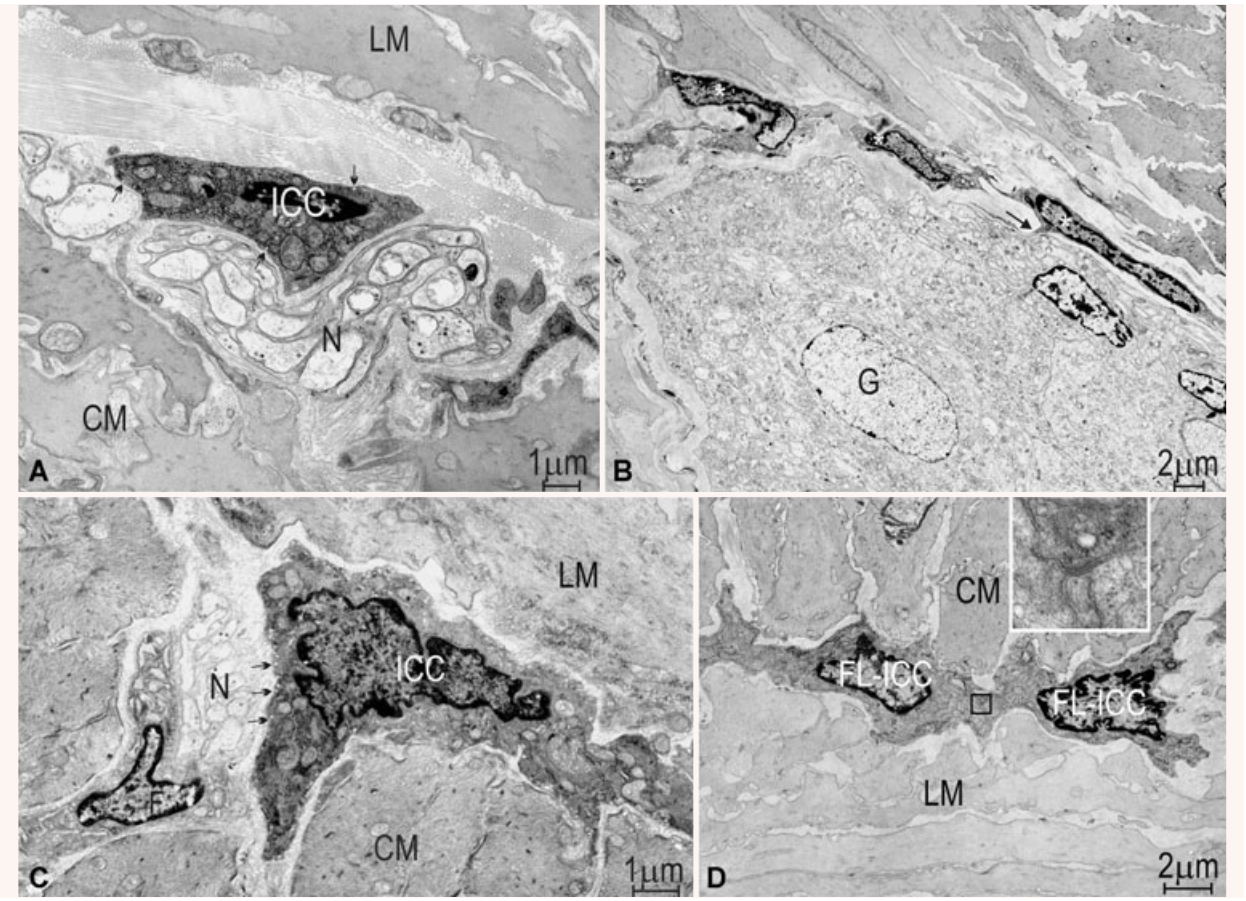

Fig. 7 Ultrastructure of interstitial cells (ICC and FL-ICC) at the Auerbach's plexus of wild-type (**a**) and Ws/Ws rat colon (**b**–**d**). (**a**) An ICC-AP (ICC) with typical ultrastructural features of ICC–electron-dense cytoplasm, abundant mitochondria and numerous caveolae (small arrows), in the wild-type rat proximal colon. The ICC was typically close to nerve bundles (N) of the Auerbach's plexus between the circular (CM) and longitudinal muscle layer (LM). (**b**). Ultrastructure at low magnification showing an overview of interstitial cells associated with Auerbach's plexus in Ws/Ws proximal colon. Abundant interstitial cells (which could not be identified at low magnification, asterisks) were located around a myenteric ganglion (G). The arrow identifies a process of an interstitial cell that is closely connected with nerve varicosities from the myenteric ganglion (G). (**c**). At higher magnification ICC-AP (ICC) can be identified in Ws/Ws proximal colon. ICC showed the same ultrastructural features as the one in figure a (small arrows indicated the caveolae) and was also close to a nerve bundle (N). A typical fibroblast (F), which has lower electron density and a large amount of rough endoplasmic reticulum in the cytoplasm, was nearby. (**d**). Two FL-ICC with fibroblast features (abundant rough endoplasmic reticulum) were connected to each other (box) in the Auerbach's plexus of Ws/Ws mid colon. There were no caveolae displayed along their cell membrane in this profile. Inset is an enlarged figure of the boxed area of (**d**), showing a gap junction between the two cells. CM and LM: circular and longitudinal muscle layers.

(Fig. 10b) in contrast to wild-type littermates where ICC-IM were abundant (Fig. 10a).

Discussion

Pacemaker functions of ICC

In the Ws/Ws colon, an almost complete lack of development of c-Kit$^+$ ICC was noted except for the development of some ICC-AP, in particular in the proximal colon based on immunohistochemical (present study and [12]) and ultrastructural data (present study). This provides structural evidence for the relationship between impairment of pacemaker activity, regular rhythmic depolarizations at 1.2 cycles/min. [12, 13], and loss of ICC-AP, in particular in the mid and distal colon. Interestingly, we did not notice a loss of the total number of all types of interstitial cells around the colonic ganglia but rather a replacement of ICC with FL-ICC. Different from regular fibroblasts in the connective tissues, these FL-ICC were located in areas normally occupied by ICC, formed gap junctions with each other as well as with adjacent smooth

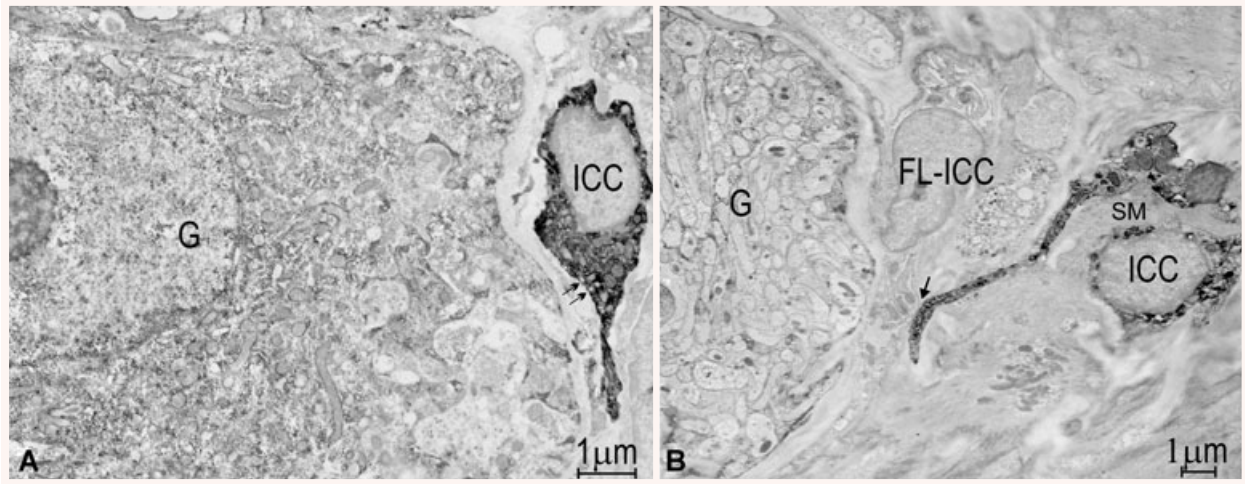

Fig. 8 c-Kit immuno EM pictures showing c-Kit$^+$ ICC in wild-type proximal colon and c-Kit$^-$ FL-ICC in Ws/Ws mid colon. (**a**) A c-Kit$^+$ ICC-AP (ICC, dark stained with DAB) situated at a ganglion in Auerbach's plexus. Many caveolae (small arrows) were located along the membrane of the c-Kit$^+$ ICC. (**b**). A c-Kit$^-$ FL-ICC was also close to a myenteric ganglion. Nearby was a c-Kit$^+$ ICC-AP (ICC, dark stained) which was crossed over by a muscle bundle (SM). The processes of ICC and FL-ICC were directly contacting each other (arrow).

muscle cells. These c-Kit$^-$ cells are similar to the FL-ICC identified in the rat stomach [22, 28, 29], and mouse small intestine [30]. Another interesting feature of FL-ICC is their SK3 positivity [31, 32]. SK3 belongs to the apamin sensitive SK Ca^{2+}-activated K^+ channel family, possibly involved in inhibitory neurotransmission [12]. These FL-ICC can be considered immature ICC and may not have developed primary pacemaker function because of a failure to develop caveolae which might harbour a crucial component of the pacemaker mechanism [33].

In *W* mutant animals, rhythmic contractile activity is sometimes observed in organs lacking pacemaker ICC. The origin of this rhythmic activity could be intrinsic to remaining ICC, as we did find c-Kit$^+$ ICC-AP in the Ws/Ws colon. It could also be due to functional activity of immature ICC or it could be associated with intrinsic, stimulus-dependent rhythmicity of smooth muscle cells. The observation of immature ICC with possible functional activity has implications for assessment of ICC injury in human disease. It is clearly advisable to evaluate ICC pathology using electron microscopy in addition to examination of c-Kit positivity [34]. Future studies might identify immunohistochemical markers of immature ICC.

In the rat colon, ICC-SMP may provide a pacemaker function in addition to ICC-AP; the ICC-SMP are associated with fast rhythmic depolarizations at 20 cycles/min. [13]. In the Ws/Ws colon, this high-frequency pacemaker activity was not evident [12] and the present study provides support for the hypothesis that absence of ICC-SMP is responsible for this. Irregular contractile activity in a frequency range similar to the high-frequency depolarization does occur in the Ws/Ws colon. This may be related to oscillatory activity associated with secondary pacemaker activity from smooth muscle cells or from immature ICC since our ultrastructural studies did show FL-ICC at the same location as ICC-SMP in wild-type colon.

Role of ICC in innervation to smooth muscle cells

ICC-IM are normally associated with nerve varicosities scattered throughout both muscle layers. In the Ws/Ws rat colon, no ICC-IM were identified but the number of fibroblasts was increased compared to wild-type rat colon. We did not identify FL-ICC at this location but we cannot confirm their absence because we may not have captured sections where gap-junctional communication would have been confirmed. This is more difficult to find within the musculature where fibroblast-like cells are scattered compared to the Auerbach's or the SMP areas where they are densely present. Since CD34$^+$/Igf1r$^+$ cells were common within the musculature, it is possible that future studies will reveal that the fibroblasts developed within the musculature and associated with nerve varicosities have more in common with FL-ICC than with common fibroblasts and that a fraction of these FL-ICC are ICC progenitor cells.

Assessment of nNOS$^+$ neurons was carried out using immunohistochemistry together with a stereological analysis that has been widely used to quantify the loss of neurons in the brain in several conditions, such as in aging [35]. This methodology has been previously used to quantify the distribution of c-Kit and nNOS$^+$ cells in the colon of Sprague-Dawley rats [23]. Both in wild-type and Ws/Ws rats, nNOS$^+$ neurons were found in the colon between circular and longitudinal muscle layers forming a network of nerve strands and ganglia. Moreover, fine fibres were found running parallel to the long axes of smooth muscle cells, especially in the circular muscle layer. The density of nNOS$^+$ neurons was not homogeneous along the colon, being highest in the mid area in both wild-type and Ws/Ws rats. The high density of nNOS$^+$ neurons in the mid colon is consistent with a strong

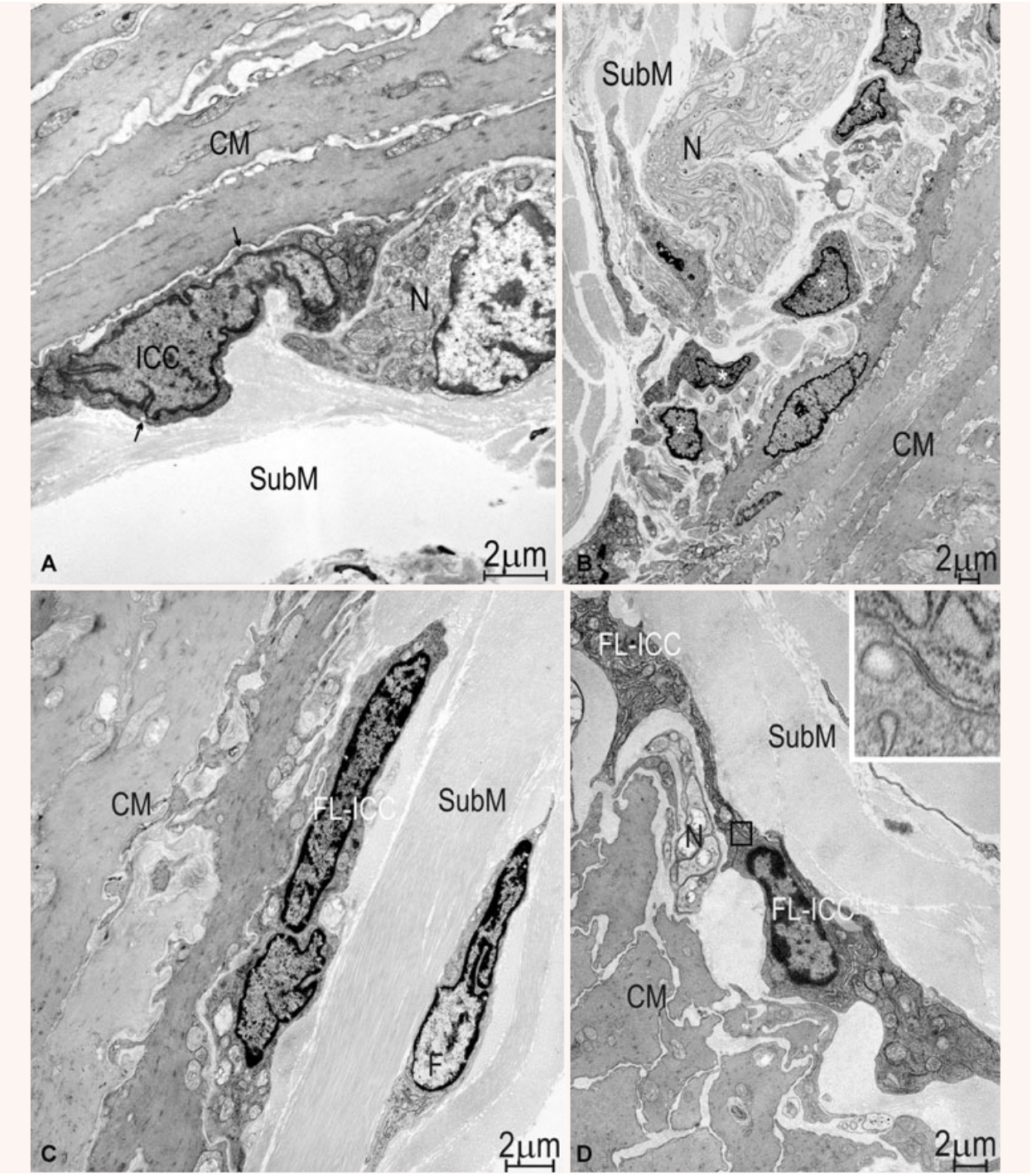

Fig. 9 Ultrastructure of ICC-SMP in wild-type rat colon (**a**) and FL-ICC at the level of the SMP of Ws/Ws colon (**b**–**d**). (**a**) An ICC-SMP (ICC) with typical ICC ultrastructural features was located along the inner margin of the circular muscle layer (CM) in wild-type proximal colon. Small arrows indicate caveolae. SubM: submucosa; N: enteric nerves. (**b**). Low magnification shows an overview of interstitial cells that could not be identified at this magnification (*) in the proximal colon of Ws/Ws rat. They were close to the nerves (N) at the SMP. (**c**). A FL-ICC with a high density of mitochondria, but without identifiable caveolae, is seen between the submucosa (SubM) and the circular muscle layer (CM) in the mid colon. A typical fibroblast (F) was nearby. (**d**). Two FL-ICC were connected (box) to each other in the distal colon. Inset shows the boxed area enlarged identifying a gap junction between the two FL-ICC. N: enteric nerves.

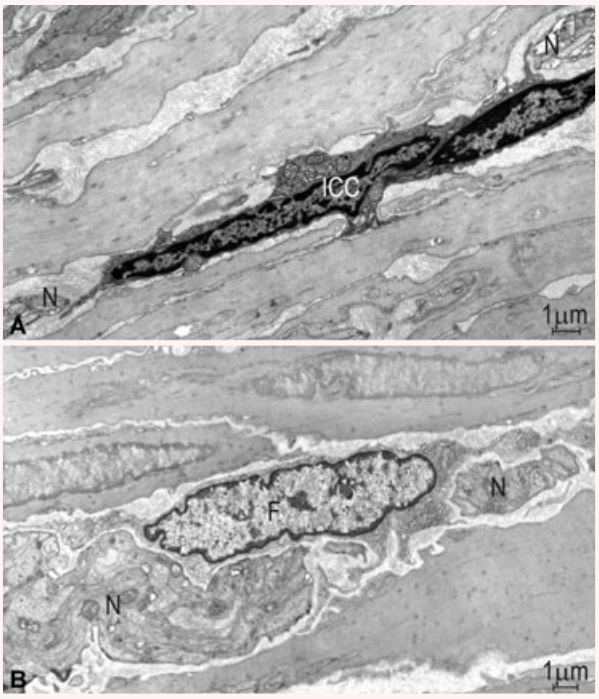

Fig. 10 ICC-IM and fibroblasts. (**a**). Abundant ICC-IM (ICC) were encountered in wild-type proximal colon identified by an electron-dense cytoplasm, numerous mitochondria in the cytoplasm and caveolae rich membranes. ICC were associated with nerve varicosities (N). (**b**) No ultrastructurally defined ICC-IM were observed in the Ws/Ws rat colon. In areas where normally ICC were found, fibroblasts (F) were located and identified as fibroblast by their high density of rough endoplasmic reticulum, and free ribosomes in the cytoplasm. N: enteric nerves.

nitrergic tone found at the same location in Sprague-Dawley rats [23]. Comparing the density of $nNOS^+$ neurons between Ws/Ws and wild-type rats, a significant decrease in the number of $nNOS^+$ neurons was shown in the mid and distal colon (35% and 29%, respectively). This decrease in the density of $nNOS^+$ neurons in mutant rats is a likely explanation for the reduction in the second (L-NNA sensitive) component of the inhibitory junction potential in these animals [12]. It is not known how a c-kit mutation affects development of nitrergic nerves. It is not likely that the development of nitrergic nerves is linked to the development of ICC [36] although it has been reported that c-kit mutant mice have a selective loss of vagal terminals in the fundus [37, 38]. The dependence of nitrergic nerves on stem cell factor-c-kit interaction is possibly indirect and may be related to c-kit dependent development of other cells such as mast cells which provide an abundance of growth factors that may be relevant under normal physiological conditions [39]. Our results demonstrate that it is important to measure the number of nNOS neurons when an impairment of the nitrergic neurotransmission is found in a specific model.

FL-ICC as immature ICC and a subset of FL-ICC as potential adult progenitor cells

ICC originate from mesenchymal progenitor cells that co-express both c-Kit and the smooth muscle specific 'smooth muscle myosin heavy chain' during embryogenesis. In the mouse, at day E14 or E15 of embryological development, ICC-AP and longitudinal smooth muscle lineages begin to diverge and at day E18, an ICC-AP network is developing [40, 41]. At birth, ultrastructurally the ICC are premature and referred to as 'ICC_{blasts}' [20, 42, 43] and are similar in all aspects (ultrastructural features, proximal location to enteric nerves and intimate connections with adjacent smooth muscle cells) to the FL-ICC described in the present paper. The network of these premature ICC is methylene blue and $c\text{-}Kit^+$. Two days after birth, the electrical pacemaker activity is fully developed [42] and structurally the ICC network is mature after weaning [20]. Adult animals with a mutation in the *c-kit* gene (referred to as *W* mutation) do not have a $c\text{-}Kit^+$ functional ICC-AP network. Embryos homozygous for the regulatory W^{banded} (W^{bd}) mutation do not express Kit in the mesenchymal progenitor cells [40]. However, at day 5 postnatal, W^{bd}/W^{bd} mice display a normal network of 'ICC' based on methylene blue staining. In another study, a mutation was introduced by gene targeting at the *W/kit* locus in mouse embryonic stem cells [44]. The *lacZ* reporter gene was inserted into the first exon of *c-kit*, thus creating a null allele, called W^{lacZ}, enabling β galactosidase expression to faithfully recapitulate the endogenous c-Kit expression. Although W^{lacZ}/W^{lacZ} embryos completely lack c-Kit protein, an apparently normal network of 'ICC' was found at birth based on β galactosidase staining, which indicates *LacZ* expression in the cells that normally express *c-kit*. Based on these two studies, one can conclude that in the absence of a fully functional c-Kit receptor, a network of cells is present at birth at the ICC location that consists of $c\text{-}Kit^-$ immature ICC. It as been generally assumed that in W mutant animals, no cellular development of certain subtypes of ICC occurred after birth leading to loss of ICC. The present study suggests that the immature ICC present at birth develop into a network of immature ICC in adult animals.

Are these networks of immature cells functional? Thuneberg studied segmental activity in 5-day-old W/W^v mice occurring at the pacemaker frequency [45]; hence, these networks of immature ICC might be viable. In adult W/W^v mice, rhythmic propulsive motor activity is also observed [6] and electrical pacing of intestinal contractions is possible [46]. It needs further study to understand the role of immature ICC in these activities since it is possible that the rhythmic contractile activity in W/W^v mice intestine is a reflection of a secondary pacemaker system in the smooth muscle layer. The assessments of these immature ICC or FL-ICC can only be done with ultrastructural studies since the cells are defined by ultrastructural features and no unique immunohistochemical features have been identified thus far.

We suggested that FL-ICC were immature ICC that might correspond to early progenitor ICC in the mouse stomach [21]. In that study $Kit_{low}/CD44+/CD34^+/Insr+/Igf1r^+$ cells were identified

by flow cytometry and resembled common embryonic precursors of ICC and smooth muscle. It is significant that Igf1r plays an important role in ICC differentiation from ICC progenitors to mature ICC [47]. Fibroblast-like cells associated with ICC are $CD34^+$ [48] and the present study shows that a subset of $CD34^+$ cells in the Ws/Ws colon are $Igf1r^+$. These $Igf1r^+/CD34^+$ cells were situated at the same locations as FL-ICC identified by electron microscopy. This leads to the hypothesis that in the adult rat colon $CD34^+$, $Igf1r^+$ FL-ICC are present that function as ICC progenitor cells and that their number is greatly increased in the Ws colon where normal development of ICC has not occurred. FL-ICC with or without progenitor function could aid in the development of motor patterns (including secondary pacemaker activity) that allow the mutant rats to survive without primary pacemaker cells [6]. Strong slow wave activity was observed in tissue cultures devoid of ICC but rich in putative ICC progenitor cells [21]. Further understanding of progenitor cells may lead to avenues of restoring primary pacemaker activity [49, 50] in tissue that have lost ICC through injury [51–54] or abnormal development [55].

In summary, it appears that in *W* mutant animals the total quantity of all types of interstitial cells does not diminish. Some ICC subtypes develop normally whereas others such as the ICC-AP and ICC-SMP in the colon develop only as immature ICC with the ultrastructural appearance of FL-ICC. FL-ICC do occur in wild-type animals, hence their number is vastly increased in W mutant animals. A subset of FL-ICC is $Igf1r^+/CD34^+$ in both wild-type and W mutant animals, and their number is markedly increased in the W mutant animals. It was recently established that progenitors of ICC in the stomach are $Igf1r^+/CD34^+$ [21]. Hence the $Igf1r^+/CD34^+$ FL-ICC are likely adult ICC progenitor cells. Whether these cells function as ICC stem cells in response to injury needs further study. It cannot be ruled out that the immature ICC have functional relevance for normal motor activity.

Acknowledgements

The following operating grants supported this research: MOP-12874 from the Canadian Institutes of Health Research; a graduate scholarship for E.J. White from the Canadian Institutes for Health Research; SAF2003–05830 and BFU2006–05055 from the Ministerio de Ciencia y Tecnologia; Leo Pharma Research Foundation, Denmark.

References

1. **Huizinga JD, Thuneberg L, Klüppel M, *et al.*** The *W/kit* gene required for interstitial cells of Cajal and for intestinal pacemaker activity. *Nature.* 1995; 373: 347–9.
2. **Ward SM, Burns AJ, Torihashi S, *et al.*** Mutation of the proto-oncogene *c-kit* blocks development of interstitial cells and electrical rhythmicity in murine intestine. *J Physiol.* 1994; 480: 91–7.
3. **Koh SD, Sanders KM, Ward SM.** Spontaneous electrical rhythmicity in cultured interstitial cells of cajal from the murine small intestine. *J Physiol.* 1998; 513: 203–13.
4. **Thomsen L, Robinson TL, Lee JCF, *et al.*** Interstitial cells of Cajal generate a rhythmic pacemaker current. *Nat Med.* 1998; 4: 848–51.
5. **Der-Silaphet T, Malysz J, Arsenault AL, *et al.*** Interstitial cells of Cajal direct normal propulsive contractile activity in the small intestine. *Gastroenterology.* 1998; 114: 724–36.
6. **Huizinga JD, Ambrous K, Der-Silaphet TD.** Co-operation between neural and myogenic mechanisms in the control of distension-induced peristalsis in the mouse small intestine. *J Physiol.* 1998; 506: 843–56.
7. **Boddy G, Willis A, Galante G, *et al.*** Sodium-, chloride-, and mibefradil-sensitive calcium channels in intestinal pacing in wild-type and W/WV mice. *Can J Physiol Pharmacol.* 2006; 84: 589–99.
8. **Liu LWC, Thuneberg L, Huizinga JD.** Cyclopiazonic acid, inhibiting the endoplasmic reticulum calcium pump, reduces the canine colon pacemaker frequency. *J Pharmacol Exp Ther.* 1995; 275: 1058–68.
9. **Liu LWC, Huizinga JD.** Electrical coupling of circular muscle to longitudinal muscle and interstitial cells of Cajal in canine colon. *J Physiol.* 1993; 470: 445–61.
10. **Langton P, Ward SM, Carl A, *et al.*** Spontaneous electrical activity of interstitial cells of Cajal isolated from canine proximal colon. *Proc Natl Acad Sci USA.* 1989; 86: 7280–4.
11. **Huizinga JD.** Motor physiology of the human colon. In: Kamm M, Lennard-Jones J, editors. Gastrointestinal transit: pathophysiology and pharmacology. Wrightson: Biomedical Publishing Ltd.; 1991. pp. 65–75.
12. **Alberti E, Mikkelsen HB, Wang XY, *et al.*** Pacemaker activity and inhibitory neurotransmission in the colon of Ws/Ws mutant rats. *Am J Physiol Gastrointest Liver Physiol.* 2007; 292: G1499–510.
13. **Pluja L, Alberti E, Fernandez E, *et al.*** Evidence supporting presence of two pacemakers in rat colon. *Am J Physiol Gastrointest Liver Physiol.* 2001; 281: G255–66.
14. **Burns AJ, Lomax AE, Torihashi S, *et al.*** Interstitial cells of Cajal mediate inhibitory neurotransmission in the stomach. *Proc Natl Acad Sci USA.* 1996; 93: 12008–13.
15. **Ward SM.** Interstitial cells of Cajal in enteric neurotransmission. *Gut.* 2000; 47: iv40–3.
16. **Suzuki H, Ward SM, Bayguinov YR, *et al.*** Involvement of intramuscular interstitial cells in nitrergic inhibition in the mouse gastric antrum. *J Physiol.* 2003; 546: 751–63.
17. **Ward SM, Sanders KM, Hirst GD.** Role of interstitial cells of Cajal in neural control of gastrointestinal smooth muscles. *Neurogastroenterol Motil.* 2004; 16: 112–7.
18. **De Lorijn F, De Jonge WJ, Wedel T, *et al.*** Interstitial cells of Cajal are involved in the afferent limb of the rectoanal inhibitory reflex. *Gut.* 2005; 54: 1107–13.
19. **Huizinga JD, Liu LW, Fitzpatrick A, *et al.*** Deficiency of intramuscular ICC increases fundic muscle excitability but does not impede nitrergic innervation. *Am J Physiol Gastrointest Liver Physiol.* 2008; 294: G589–94.
20. **Faussone-Pellegrini MS.** Cytodifferentiation of the interstitial cells of Cajal related to the myenteric plexus of mouse intestinal muscle coat. An E.M. study from foetal to adult life. *Anat Embryol.* 1985; 171: 163–9.

21. **Lorincz A, Redelman D, Horvath VJ, *et al.*** Progenitors of interstitial cells of cajal in the postnatal murine stomach. *Gastroenterology.* 2008; 134: 1083–93.
22. **Ishikawa K, Komuro T, Hirota S, *et al.*** Ultrastructural identification of the c-kit-expressing interstitial cells in the rat stomach: a comparison of control and Ws/Ws mutant rats. *Cell Tissue Res.* 1997; 289: 137–43.
23. **Alberti E, Mikkelsen HB, Larsen JO, *et al.*** Motility patterns and distribution of interstitial cells of Cajal and nitrergic neurons in the proximal, mid- and distal-colon of the rat. *Neurogastroenterol Motil.* 2005; 17: 133–47.
24. **Toth C, Brussee V, Martinez JA, *et al.*** Rescue and regeneration of injured peripheral nerve axons by intrathecal insulin. *Neuroscience.* 2006; 139: 429–49.
25. **Gundersen HJ.** Stereology of arbitrary particles. A review of unbiased number and size estimators and the presentation of some new ones, in memory of William R. Thompson. *J Microsc.* 1986; 143: 3–45.
26. **Larsen J.O.** Qualitative and quantitative assessment of peripheral nerves with implanted nerve cuff electrodes. Faculty of Health Sciences, Denmark: University of Aarhus; 1998.
27. **Mayhew TM.** An efficient sampling scheme for estimating fibre number from nerve cross sections: the fractionator. *J Anat.* 1988; 157: 127–34.
28. **Horiguchi K, Komuro T.** Ultrastructural characterization of interstitial cells of Cajal in the rat small intestine using control and Ws/Ws mutant rats. *Cell Tissue Res.* 1998; 293: 277–84.
29. **Mitsui R, Komuro T.** Distribution and ultrastructure of interstitial cells of Cajal in the gastric antrum of wild-type and Ws/Ws rats. *Anat Embryol.* 2003; 206: 453–60.
30. **Horiguchi K, Komuro T.** Ultrastructural observations of fibroblast-like cells forming gap junctions in the W/W(nu) mouse small intestine. *J Auton Nerv Syst.* 2000; 80: 142–7.
31. **Fujita A, Takeuchi T, Jun H, *et al.*** Localization of Ca2+-activated K+ channel, SK3, in fibroblast-like cells forming gap junctions with smooth muscle cells in the mouse small intestine. *J Pharmacol Sci.* 2003; 92: 35–42.
32. **Vanderwinden JM, Rumessen JJ, de Kerchove dA Jr, *et al.*** Kit-negative fibroblast-like cells expressing SK3, a Ca2+-activated K+ channel, in the gut musculature in health and disease. *Cell Tissue Res.* 2002; 310: 349–58.
33. **Daniel EE, El-Yazbi A, Cho WJ.** Caveolae and calcium handling, a review and a hypothesis. *J Cell Mol Med.* 2006; 10: 529–44.
34. **Zarate N.** Interstitial cells of Cajal: key players in gastrointestinal motor disorders. Barcelona: Autonomous University of Barcelona; 2008.
35. **Long JM, Mouton PR, Jucker M, *et al.*** What counts in brain aging? Design-based stereological analysis of cell number. *J Gerontol A Biol Sci Med Sci.* 1999; 54: B407–17.
36. **Young HM, Ciampoli D, Southwell BR, *et al.*** Origin of interstitial cells of Cajal in the mouse intestine. *Dev Biol.* 1996; 96: 97–107.
37. **Fox EA, Phillips RJ, Martinson FA, *et al.*** C-Kit mutant mice have a selective loss of vagal intramuscular mechanoreceptors in the forestomach. *Anat Embryol.* 2001; 204: 11–26.
38. **Powley TL, Wang XY, Fox EA, *et al.*** Ultrastructural evidence for communication between intramuscular vagal mechanoreceptors and interstitial cells of Cajal in the rat fundus. *Neurogastroenterol Motil.* 2008; 20: 69–79.
39. **Maurer M, Theoharides T, Granstein RD, *et al.*** What is the physiological function of mast cells? *Exp Dermatol.* 2003; 12: 886–910.
40. **Klüppel M, Huizinga JD, Malysz J, *et al.*** Developmental origin and Kit-dependent development of the interstitial cells of Cajal in the mammalian small intestine. *Dev Dyn.* 1998; 211: 60–71.
41. **Ward SM, Sanders KM.** Physiology and pathophysiology of the interstitial cell of Cajal: from bench to bedside. I. Functional development and plasticity of interstitial cells of Cajal networks. *Am J Physiol Gastrointest Liver Physiol.* 2001; 281: G602–11.
42. **Liu LWC, Thuneberg L, Huizinga JD.** Development of pacemaker activity and interstitial cells of Cajal in the neonatal mouse small intestine. *Dev Dyn.*1998; 213: 271–82.
43. **Torihashi S, Ward SM, Nishikawa S, *et al.*** *c-kit*-dependent development of interstitial cells and electrical activity in the murine gastrointestinal tract. *Cell Tissue Res.* 1995; 280: 97–111.
44. **Bernex F, De SP, Kress C, *et al.*** Spatial and temporal patterns of c-kit-expressing cells in $W^{lacZ}/+$ and W^{lacZ}/W^{lacZ} mouse embryos. *Development.* 1996; 122: 3023–33.
45. **Thuneberg L, Peters S.** Toward a concept of stretch-coupling in smooth muscle. I. Anatomy of intestinal segmentation and sleeve contractions. *Anat Rec.* 2001; 262: 110–24.
46. **Daniel EE, Willis A, Cho WJ, *et al.*** Comparisons of neural and pacing activities in intestinal segments from W/W++ and W/W(V) mice. *Neurogastroenterol Motil.* 2005; 17: 355–65.
47. **Horvath VJ, Vittal H, Lorincz A, *et al.*** Reduced stem cell factor links smooth myopathy and loss of interstitial cells of Cajal in murine diabetic gastroparesis. *Gastroenterology.* 2006; 130: 759–70.
48. **Vanderwinden JM, Rumessen JJ, De Laet MH, *et al.*** $CD34^+$ cells in human intestine are fibroblasts adjacent to, but distinct from, interstitial cells of Cajal. *Lab Invest.* 1999; 79: 59–65.
49. **Ordog T.** Interstitial cells of Cajal in diabetic gastroenteropathy. *Neurogastroenterol Motil.* 2008; 20: 8–18.
50. **Huizinga JD, White EJ.** Progenitor cells of interstitial cells of Cajal: on the road to tissue repair. *Gastroenterology.* 2008; 134: 1252–4.
51. **Wang XY, Zarate N, Soderholm JD, *et al.*** Ultrastructural injury to interstitial cells of Cajal and communication with mast cells in Crohn's disease. *Neurogastroenterol Motil.* 2007; 19: 349–64.
52. **Boeckxstaens GE, Rumessen JJ, de Wit L, *et al.*** Abnormal distribution of the interstitial cells of cajal in an adult patient with pseudo-obstruction and megaduodenum. *Am J Gastroenterol.* 2002; 97: 2120–6.
53. **Rumessen JJ, Vanderwinden JM.** Interstitial cells in the musculature of the gastrointestinal tract: Cajal and beyond. *Int Rev Cytol.* 2003; 229: 115–208.
54. **Der T, Bercik P, Donnelly G, *et al.*** Interstitial cells of Cajal and inflammation-induced motor dysfunction in the mouse small intestine. *Gastroenterology.* 2000; 119: 1590–9.
55. **Vanderwinden JM, Liu H, Menu R, *et al.*** The pathology of infantile hypertrophic pyloric stenosis after healing. *J Pediatr Surg.* 1996; 31: 1530–4.